

A Second Set of RATAN-600 Observations of Giant Radio Galaxies

M. L. Khabibullina¹, O. V. Verkhodanov¹, M. Singh²,
A. Pirya², S. Nandi², and N. V. Verkhodanova¹

¹*Special Astrophysical Observatory, Russian Academy of Sciences,
Nizhnii Arkhyz, Karachaevo-Cherkesskaya Republic, 357169 Russia*

²*Aryabhata Research Institute of Observational Sciences,
Manora Peak, Nainital, 263129 Uttarakhand, India*

Received September 2, 2010; in final form, November 20, 2010

Abstract—Results of RATAN-600 centimeter-wavelength flux-density measurements of the extended components in five giant radio galaxies are reported. The spectra of the components of these radio galaxies have been constructed using the data of the WENSS, NVSS, and GB6 surveys together with new RATAN-600 data. Spectral indices in the studied frequency range have been calculated.

DOI: 10.1134/S1063772911050027

1. INTRODUCTION

In 2008, we initiated a program of observations of giant radio galaxies (GRGs) on the RATAN-600 radio telescope. In December 2008, we conducted a first set of observations and obtained integrated spectra for the components in seven radio galaxies: GRG 0139+3957, GRG 0912+3510, GRG 1032+2759, GRG 1343+3758, GRG 1400+3017, GRG 1453+3308, GRG 1552+2005, and GRG 1738+3733. These observations [1] showed that the radio spectral indices of the components of these radio galaxies differ considerably. The form of the spectra also differs, from very steep, as in GRG 0139+3957, to fairly flat, as in the components of GRG 1738+3733.

Radio observations of GRGs can help elucidate the origin of objects with such giant sizes, which is not yet entirely clear. According to the generally accepted definition, GRGs are radio sources with linear dimensions larger than 1 Mpc. They are the largest objects in the visible Universe, and it is possible that they played a special role in the formation of the large-scale structure. The large sizes of GRGs also suggest that these sources must be at a late stage in their evolution. Models of radio sources [2, 3] predict a change in the radio luminosity and linear dimensions of powerful radio sources with time. According to these models, GRGs should be very old objects (with ages $>10^8$ years) and should presumably be in a lower density medium compared to smaller sources with comparable radio luminosities [4]. Their analysis of

radio and optical data (SDSS, APM) for radio galaxies and quasars led Komberg and Pashchenko [5] to conclude that, apart from environment effects, the sizes of giant radio sources could be explained by the presence of a population of long-lived, radio-loud active galactic nuclei, which, in turn, can evolve to GRGs. Multifrequency observations [6] showed that the spectral ages of GRGs are greater than is expected from evolutionary models. As was noted in [7], such radio galaxies could influence the formation of galaxies, since the pressure of the gas outflowing from a radio source could compress cold gas clouds and initiate the development of stars, on the one hand, and stop the formation of a galaxy, on the other hand. Note that several teams [8–17] are investigating the origin of GRGs and physical processes in these radio sources. However, thus far, there is no definite solution to this problem.

Our analysis of the spectra of radio galaxies in [1] led us to the conclusion that the center-to-edge variation of the spectral indices for GRGs is due to a change in the particle energy in the components (this was also noted earlier in [9]). This change is due to pressure variations in the surrounding streaming gas; i.e., to a change in the environment that depends on distance from the host galaxy. However, general conclusions will be more significant in an integrated approach to the GRG population as a whole. An important stage in studying the origin of the large sizes of GRGs is a comparative analysis of the properties of “ordinary” radio galaxies, also carried out in the framework of this project [18–20]. Earlier, Soboleva

Table 1. Main parameters of the GRGs from the observing proposal

Source	Coordinates RA + Dec (J2000.0) hhmmss + ddmms	Redshift	Type	Angular size, arcmin	Flux density (1.4 GHz), mJy
GRG 0452+5204	045253 + 520447	0.109	I	9.7	2869.1
GRG 0751+4231	075109 + 423124	0.203	II	6.0	162.3
GRG 0929+4146	092911 + 414646	0.365	II	6.6	165.5
GRG 1216+4159	121610 + 415927	0.243	II	5.2	415.5
GRG 1521+5105	152115 + 510501	(0.37)	II	4.3	1197.5
GRG 1918+516	191923 + 514334	0.284	II	7.3	920
GRG 2103+6456	210314 + 645655	0.215	II	4.8	119.7

[21] observed arcminute-size radio galaxies at centimeter and decimeter wavelengths on the RATAN-600, and found that their morphological structures have virtually identical spectral indices. Therefore, studies of the remaining objects of the GRG sample will enable us to supplement available information on the radio spectra of this population.

We also noted that the millimeter-wavelength flux densities of the studied GRG components estimated from extrapolated spectra are above 0.6 mJy [1]. This could be relevant for estimates of the contributions of various effects to anisotropy of the cosmic microwave background (CMB) on scales of galaxy clusters. Thus, knowledge of the spectral indices, shapes, and orientations of GRGs will facilitate taking into account features of regions with sizes of up to $10'$ on maps of the CMB anisotropy [22].

In the current paper, we continue our RATAN-600 study of this GRG sample and present new observations of these radio galaxies at centimeter and decimeter wavelengths.

2. RATAN-600 DATA

2.1. RATAN-600 Observations

The observations of a new subsample of GRGs were conducted on the Southern sector of the RATAN-600 in the first ten days of January 2010. The observations were made using continuum radiometers of the first feed for wavelengths of 1.38, 2.7, 3.9, 6.25, 13, and 31 cm. As in [1], owing to the poor interference conditions during the observations, data suitable for the analysis were obtained in only four bands: 2.7, 3.9, 6.25, and 13 cm. At the observed elevations, the beamwidths in the central cross section were $25''$, $36''$, $57''$, and $119''$, respectively. At 6.25 and 13 cm, we used subchannels of the spectrum analyzer that enabled us to effectively

suppress interference. The observed sources are listed in Table 1, and a log of the observations is in Table 2. Note that GRG 2103+64 was observed nine times in this set of observations; however, we could not achieve a signal-to-noise ratio sufficient to detect this source.

2.2. Data Processing

To reduce the flux densities to the international scale [23], we observed calibration sources from the standard RATAN-600 list [24, 25]. The transit curves of the sources were analyzed in the FADPS processing system [26, 27]. We first subtracted a low-frequency trend with a smoothing window of $8'$ from the transit records of the sources. To estimate the flux densities, we used the integrated values under the RATAN-600 beam transit curves approximated by a set of Gaussians. The noise levels in the single-transit records at 1.38, 2.7, 3.9, 6.25, and 13 cm at

Table 2. Observed GRG areas

Source	Coordinates of the center of the observed area RA + Dec (J2000.0) (hhmmss + ddmms)	N_t
GRG 0452+5204	045343.7 + 520556	11
GRG 0751+4231	075153.9 + 422945	10
GRG 0929+4146	092951.8 + 414353	10
GRG 1216+4159	121641.4 + 415545	11
GRG 1521+5105	152132.5 + 510232	7
GRG 2103+6456	210322.1 + 645929	9

Central cross sections were done for all objects. N_t is the number of transits.

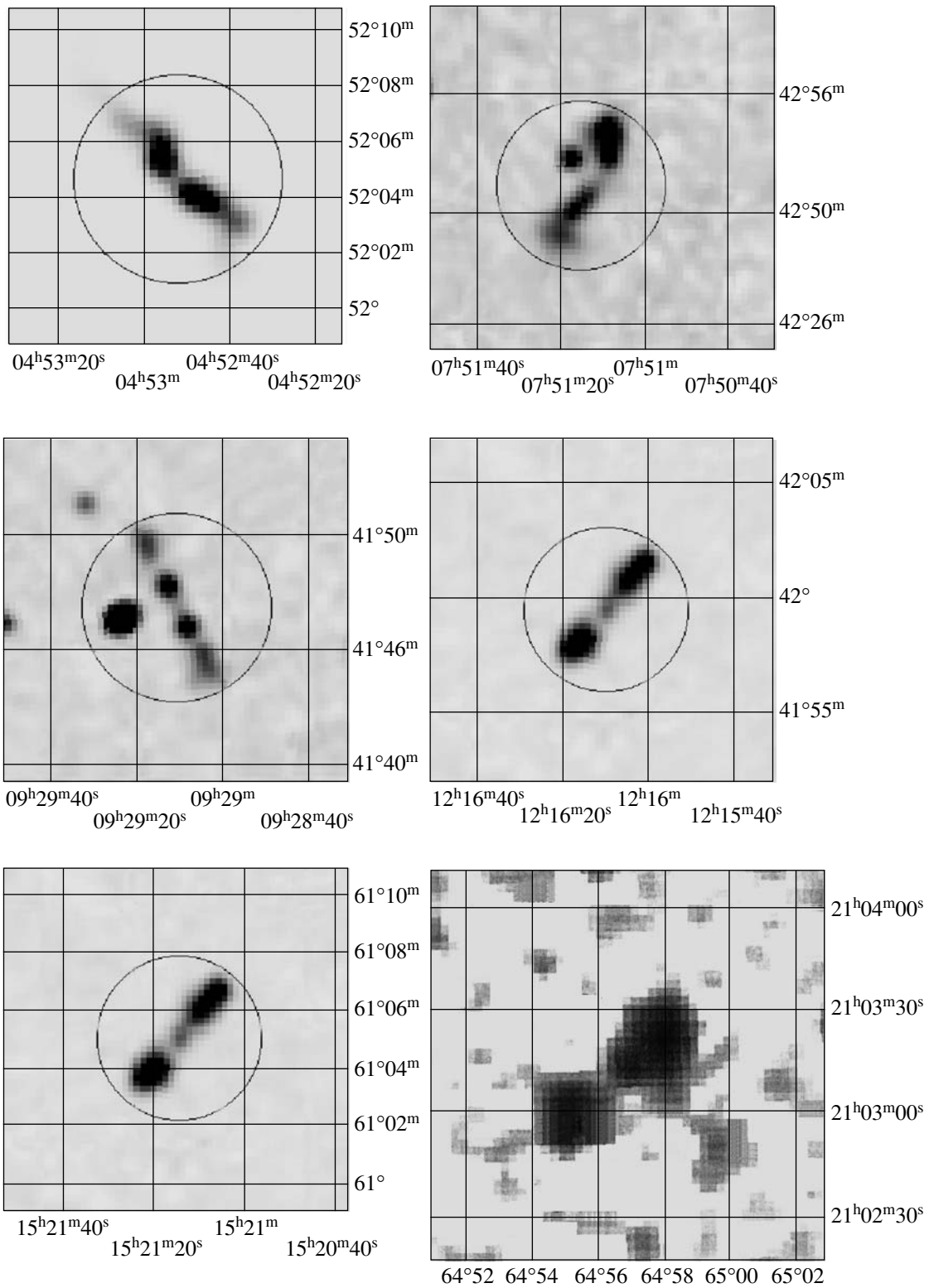


Fig. 1. NVSS radio images of GRGs. The circles denote the objects observed on the RATAN-600.

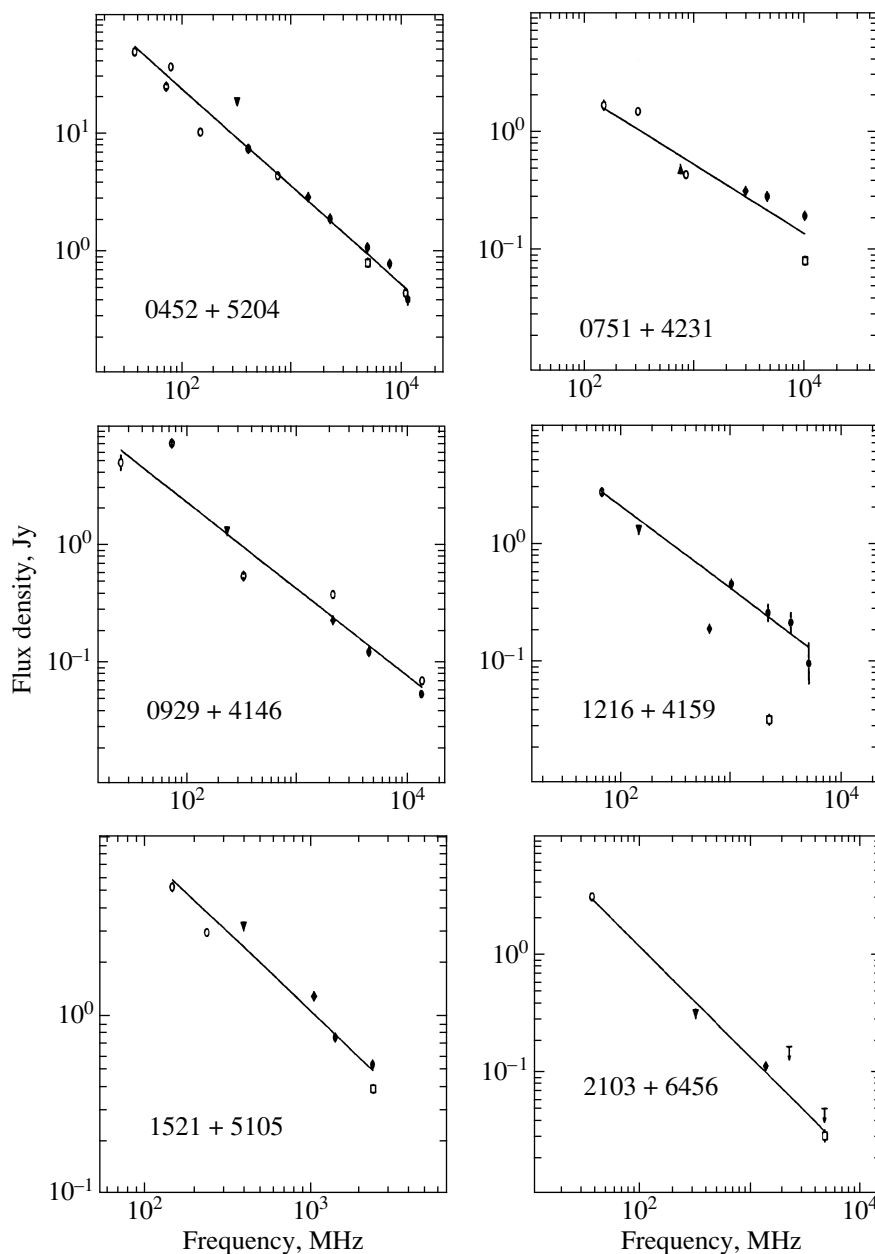


Fig. 2. Radio spectra of the GRGs plotted with data from the RATAN-600, NVSS, WENSS, GB6 (Table 3), etc. observations. The RATAN-600 data are shown by filled circles.

an elevation of 82° were 17.2, 8.9, 18.1, 10.7, and $96.6 \text{ mK/s}^{1/2}$, respectively. Table 3 lists our flux-density measurements at 2.7, 3.9, 6.25, and 13 cm, together with the integrated flux densities for the measured sources computed from the 21-cm maps of the NRAO VLA Sky Survey (NVSS, USA) [28] and the 92-cm data of the Westerbork Northern Sky Survey (WENSS, the Netherlands) [29]. Figure 1 presents the maps of the sources. To identify the objects and estimate their parameters, we also used the CATS database [30, 31]. Among the CATS

catalogs, we found identifications in the GB6 [32], VLSS [33], 6C [34], 7C [35], 8C [36], Texas [37], and B3 [38] surveys.

GRG 0452+5204 and GRG 0751+4231 were observed at 2.7 and 3.9 cm in a beam-switching mode. To take into account the probable flux-density decrease of an extended object in this observing mode, we modeled the transit of the sources across the two horns. Our modeling included calculation of the two-dimensional RATAN-600 beam at the observed wavelength using the method of Korzhavin [39] and

Table 3. Integrated flux densities (in mJy), RATAN-600, WENSS, and NVSS data

Source name	2.7 cm RATAN	3.9 cm RATAN	6.25 cm RATAN	13.5 cm RATAN	6.2 cm GB6	21 cm NVSS	92 cm WENSS
GRG 0452+5204	417	827	1141	1984	844	3003	18 760
GRG 0751+4231	103	227	274	476	35	202	1365
GRG 0929+4146	–	–	215	315	91	200	1560
GRG 1216+4159	–	–	123	207	77	264	1604
GRG 1521+5105	–	–	317	549	377	747	4903
GRG 2103+6456	–	–	<54	<180	32	124	337

the FADPS system [26], convolution with the components of the observed source, and calculation of a model transit across the RATAN-600 beam. The corrections to the integrated flux densities of extended radio sources in the modeled beam-switching mode were included in our analysis of the actual observations.

The flux-density uncertainties for the RATAN-600 data were estimated from the noise levels, and

Table 4. Fits for the GRG radio continuum spectra from 92 to 2.7 cm

Source name	Radio spectrum
GRG 0452+5204	$3.054 - 0.829x$
GRG 0751+4231	$1.971 - 0.697x$
GRG 0929+4146	$1.330 - 0.583x$
GRG 1216+4159	$2.288 - 0.882x$
GRG 1521+5105	$2.233 - 0.731x$
GRG 2103+6456	$1.942 - 0.923x$

Table 5. Integrated flux densities $S_{3\text{ mm}}$ of the GRGs at 3 mm estimated from the fits at centimeter and decimeter wavelengths

Source name	$S_{3\text{ mm}}$, mJy
GRG 0452+5204	81
GRG 0751+4231	31
GRG 0929+4146	26
GRG 1216+4159	8
GRG 1521+5105	38
GRG 2103+6456	2

were 2 mJy at 2.7 cm, 4 mJy at 3.9 cm, 5 mJy at 6.25 cm, and 52 mJy at 13 cm.

2.3. Spectra

Using our measurements, we plotted the the integrated radio spectra for the six studied sources. We parametrized these spectra using the formula $\log S(\nu) = A + Bx + Cf(x)$, where S is the flux density in Jy, x the logarithm of the frequency ν in MHz, and $f(x)$ one of the following functions: $\exp(-x)$, $\exp x$, or x^2 . We used the “spg” system for the analysis of the spectra [40]. Figure 2 shows the GRG spectra. Table 4 presents the analytical fits for the continuum spectra of the studied GRGs.

3. DISCUSSION

We have observed five GRGs for the first time and measured their flux densities using the RATAN-600 radiometer complex. We have calculated the spectral indices of the GRGs as the slopes of the tangents to the approximating curve for the integrated spectrum at a given frequency. Table 3 lists the flux densities measured at 2.7, 3.9, 6.25, and 13 cm, and Table 4 the spectral indices, equal to the coefficients of the argument x . The RATAN-600 data for GRG 0751+4231 lie above the GB6 and NVSS data. The object from the GB6 catalog is virtually pointlike; this explains the low level of its catalog flux. It is most likely that the level of the NVSS flux density has the same origin, since integrating over the peak values results in the incomplete detection of weak diffuse emission.

The radio source observed on RATAN-600 in the area of GRG 0929+4146 consists of two radio galaxies: GRG 0929+4146 proper, as a multi-component object extended along a line, and a FR II double radio source with coordinates $\alpha = 09^{\text{h}}29^{\text{m}}24^{\text{s}}$, $\delta = +41^{\circ}46'18''$ that merges into a single extended object at the left, near GRG 0929+4146 (Fig. 1). The

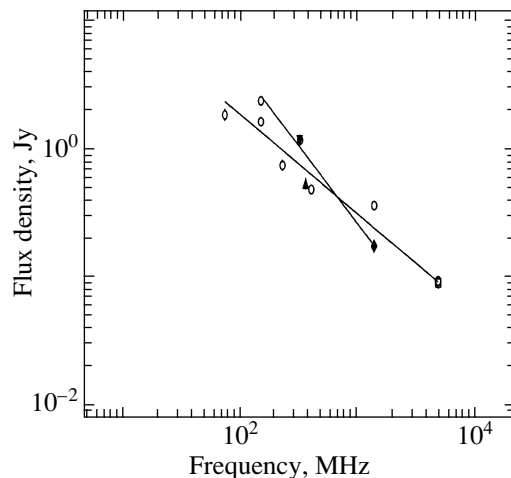


Fig. 3. Integrated radio spectra of the radio galaxies (RATAN-600 observations): GRG 0929+4146, which has a steeper spectrum, and the ordinary double radio galaxy J092924+414618.

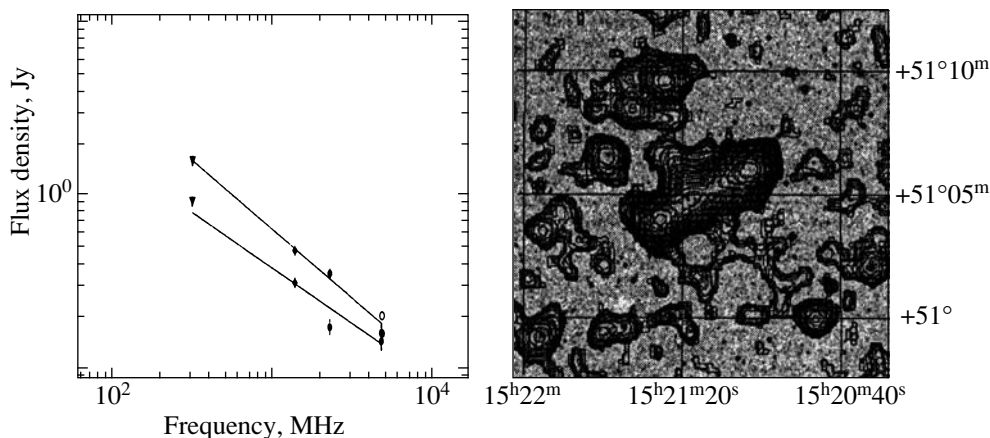


Fig. 4. Left: radio spectra of the components of GRG 1521+5105, with the RATAN-600 data shown as filled circles. Right: NVSS radio image of GRG 1521+5105 (at the map center), overlaid on the DSS optical image.

RATAN-600 does not resolve these radio galaxies in a meridian transit; thus, Fig. 2 presents the total spectrum. Using the NVSS, WENSS, and 7C data, we have plotted separate spectra for each of the radio galaxies (Fig. 3). The integrated radio spectrum for GRG 0929+4146 alone is approximated as $y = 3.046 - 1.208x$, and the spectrum of the neighboring radio galaxy is $y = 1.818 - 0.774x$, with a smaller slope demonstrating that the RATAN-600 observations at short wavelengths are dominated by the radio emission from J092924+414618.

We resolved GRG 1521+5105 into two components, whose spectra are presented in Fig. 4. The integrated flux densities for one component (J152103+510600) were 368 mJy at 13 cm and 167 mJy at 6.25 cm, whereas they were 181 mJy at 13 cm and 150 mJy at 6.25 cm for the other

component (J152125+510401). The functions fitting the radio spectra of the components are $y = 2.226 - 0.800x$ and $y = 1.537 - 0.645x$, respectively. GRG 1521+5105, which is identified with the galaxy SDSS J152114.55+510500.9 and has the photometric redshift $z = 0.37$ (NED data¹), is projected against the outskirts of the cluster NSCS J152018+505306, with redshift $z = 0.52$ (NED), at an angular distance of 15' from its center. However, there are more than 1700 galaxies (NED data) and a great number of radio sources within 10' of the radio galaxy (Fig. 4). Due to the lack of redshifts for the overwhelming majority of these, it is difficult to judge whether there could be a physical

¹<http://nedwww.ipac.caltech.edu>.

association of GRG 1521+5105 with any group of galaxies. However, the rich environment of this radio galaxy stimulates additional interest in searching for the origin of its giant size.

In addition, as in our previous work [1], we have estimated the contribution of the observed GRGs to the microwave background. We used the RATAN-600 data and the updated GRG spectra to calculate the integrated flux densities at millimeter wavelengths, listed in Table 5. The contribution of the studied giant radio sources on scales of galaxy clusters exceeds 1 mJy, and could be an important confusion factor in distinguishing components of the microwave background in the given sky regions on the given scales.

We envisage further accumulation of new data, including compiling lists of new GRGs and observations on the RATAN-600.

ACKNOWLEDGMENTS

The authors thank Yu.V. Sotnikova for help with the RATAN-600 observations. This research has made use of the NASA/IPAC Extragalactic Database (NED), which is operated by the Jet Propulsion Laboratory, California Institute of Technology, under contract with the National Aeronautics and Space Administration. We have also used the CATS database² [30, 31] and FADPS system for processing radio astronomy data³ [26, 27]. We are deeply grateful to R.D. Dagkesamanskiĭ for valuable comments on the manuscript. This work was supported by the Program of State Support of Leading Scientific Schools of the Russian Federation, the Russian Foundation for Basic Research (project 09-02-92659-IND, 09-02-00298, and 08-02-00486), and the Dynasty Foundation of Nonprofit Programs.

REFERENCES

1. M. L. Khabibullina, O. V. Verkhodanov, M. Singh, et al., *Astron. Zh.* **87**, 627 (2010) [*Astron. Rep.* **54**, 571 (2010)] arXiv: 1009.4539 [astro-ph] (2010).
2. C. R. Kaiser, J. Dennett Thorpe, and P. Alexander, *Mon. Not. R. Astron. Soc.* **292**, 723 (1997).
3. K. Blundell, S. Rawlings, and C. J. Willott, *Astron. J.* **117**, 677 (1999).
4. C. R. Kaiser and P. Alexander, *Mon. Not. R. Astron. Soc.* **302**, 515 (1999).
5. B. L. Komberg and I. N. Pashchenko, *Astron. Zh.* **86**, 1163 (2009) [*Astron. Rep.* **53**, 1086 (2009)]; arXiv:0901.3721 [astro-ph] (2009).
6. K.-H. Mack, U. Klein, C. P. O’Dea, et al., *Astron. Astrophys.* **329**, 431 (1998).
7. M. Jamrozy, J. Machalski, K.-H. Mack, and U. Klein, *Astron. Astrophys.* **433**, 467 (2005).
8. A. P. Schoenmakers, K.-H. Mack, A. G. de Bruyn, et al., *Astron. Astrophys. Suppl. Ser.* **146**, 293 (2000).
9. A. P. Schoenmakers, A. G. de Bruyn, H. J. A. Roettgering, and H. van der Laan, *Astron. Astrophys.* **374**, 861 (2001).
10. L. Lara, I. Marquez, W. D. Cotton, et al., *Astron. Astrophys.* **378**, 826 (2001).
11. L. Lara, G. Giovannini, W. D. Cotton, et al., *Astron. Astrophys.* **421**, 899 (2004).
12. L. Saripalli, R. W. Hunstead, R. Subrahmanyam, and E. Boyce, *Astron. J.* **130**, 896 (2005).
13. C. Konar, D. J. Saikia, C. H. Ishwara-Chandra, and V. K. Kulkarni, *Mon. Not. R. Astron. Soc.* **355**, 845 (2004).
14. C. Konar, M. Jamrozy, D. J. Saikia, and J. Machalski, *Mon. Not. R. Astron. Soc.* **383**, 525 (2008).
15. M. Jamrozy, C. Konar, J. Machalski, and D. J. Saikia, *Mon. Not. R. Astron. Soc.* **385**, 1286 (2008).
16. J. Machalski, M. Jamrozy, S. Zola, and D. Koziel, *Astron. Astrophys.* **454**, 85 (2006).
17. S. Nandi, A. Pirya, S. Pal, et al., *Mon. Not. R. Astron. Soc.* **404**, 433 (2010); arXiv:1001.3998 [astro-ph] (2010).
18. M. L. Khabibullina and O. V. Verkhodanov, *Astrophys. Bull.* **64**, 123 (2009); arXiv:0911.3741 [astro-ph] (2009).
19. M. L. Khabibullina and O. V. Verkhodanov, *Astrophys. Bull.* **64**, 340 (2009); arXiv:0911.3752 [astro-ph] (2009).
20. O. V. Verkhodanov and M. L. Khabibullina, *Pis’ma Astron. Zh.* **36**, 9 (2010) [*Astron. Lett.* **36**, 7 (2010)]; arXiv:1003.0577 [astro-ph] (2010).
21. N. S. Soboleva, *Astrofiz. Issled. (Izv. Spets. Astrofiz. Observ.)* **14**, 50 (1981).
22. O. V. Verkhodanov, M. L. Khabibullina, M. Singh, et al., in *Problems of Practical Cosmology, Proceedings of the Internat. Conference, 23–27 June, 2008, St.-Petersburg*, Ed. by Yu. V. Baryshev, I. N. Taganov, and P. Teerikorpi (Russian Geograph. Soc., St.-Petersburg, 2008), v. 2, p. 247.
23. J. W. M. Baars, R. Genzel, I. I. K. Pauliny-Toth, and A. Witzel, *Astron. Astrophys.* **61**, 99 (1977).
24. K. D. Aliakberov, M. G. Mingaliev, M. N. Nau-gol’naya, et al., *Astrofiz. Issled. (Izv. Spets. Astrofiz. Observ.)* **19**, 60 (1985).
25. S. A. Trushkin, *Handbook of Radio Continuum observer*, http://w0.sao.ru/hq/iran/manuals/ratan_manual.html (2000).
26. O. V. Verkhodanov, B. L. Erukhimov, M. L. Monosov, et al., *Bull. Spec. Astrophys. Observ.* **36**, 132 (1993).
27. O. V. Verkhodanov, in *Astronomical Data Analysis Software and Systems VI*, Ed. by G. Hunt and H. E. Payne, ASP Conf. Ser. **125**, 46 (1997).
28. J. J. Condon, W. D. Cotton, E. W. Greisen, et al., *Astron. J.* **115**, 1693 (1998).
29. R. B. Rengelink, Y. Tang, A. G. de Bruyn, et al., *Astron. Astrophys. Suppl. Ser.* **124**, 259 (1997).

²<http://cats.sao.ru>.

³http://sed.sao.ru/~vo/fadps_e.html.

30. O. V. Verkhodanov, S. A. Trushkin, H. Andernach, and V. N. Chernenkov, *Bull. Spec. Astrophys. Observ.* **58**, 118 (2005); arXiv:0705.2959 [astro-ph] (2007).
31. O. V. Verkhodanov, S. A. Trushkin, H. Andernach, and V. N. Chernenkov, *Data Sci. J.* **8**, 34 (2009), arXiv: 0901.3118.
32. P. C. Gregory, W. K. Scott, K. Douglas, and J. J. Condon, *Astrophys. J. Suppl. Ser.* **103**, 427 (1996).
33. A. S. Cohen, W. M. Lane, W. D. Cotton, et al., *Astron. J.* **134**, 1245 (2007).
34. S. E. G. Hales, C. R. Masson, P. Warner, et al., *Mon. Not. R. Astron. Soc.* **262**, 1057 (1993).
35. J. M. W. Riley, E. M. Waldram, and J. M. Riley, *Mon. Not. R. Astron. Soc.* **306**, 31 (1999).
36. S. E. G. Hales, E. M. Waldram, N. Rees, and P. J. Warner, *Mon. Not. R. Astron. Soc.* **274**, 447 (1995).
37. J. N. Douglas, F. N. Bash, F. A. Bozyan, et al., *Astron. J.* **111**, 1945 (1996).
38. A. Ficarra, G. Grueff, and G. Tomassetti, *Astron. Astrophys. Suppl. Ser.* **59**, 255 (1985).
39. A. N. Korzhavin, *Astrofiz. Issled. (Izv. Spets. Astrofiz. Observ.)* **9**, 71 (1977).
40. O. V. Verkhodanov, in *Proceedings of 27th Radioastron. Conference on Problems of Modern Radioastronomy* (IPA RAN, St.-Petersburg, 1997), vol. 1, p. 322.

Translated by G. Rudnitskii